Transcriptome analysis of the testes of male chickens with high and low sperm motility

Zhenwei Du [*,†], WenTing Li,[*,†] Cong Liu,[*,†] ChunXiu Wang,[*] DongXue Wang,[*,†] ShuaiPeng Zhu,[*,†] XiangTao Kang,[*,†] RuiRui Jiang,[*,†] LeKun Deng,[*] DongHua Li,[*,†] and GuiRong Sun [*,†,1]

[*]College of Animal Science and Technology, Henan Agricultural University, Zhengzhou 450046, China; and [†]Henan Key Laboratory for Innovation and Utilization of Chicken Germplasm Resources, Zhengzhou, 450046, China

ABSTRACT The reproductive performance of chicken breeders has significant economic importance in the poultry industry, and sperm motility is an indicator of reproductive performance. This study performed RNA-seq of the testes of *Gushi* chicken roosters with high and low sperm motility and identified differentially expressed RNAs involved in sperm motility. RNA-seq analysis showed that 73 and 67 differentially expressed mRNAs were up- and downregulated, and 47 and 56 differentially expressed long non-coding RNAs were up- and downregulated, respectively. The genes related to sperm motility and spermatogenesis included *KIFC1, KCNK2,* and *REC8.* Functional enrichment analysis revealed that the pathways related to sperm motility included oxidative phosphorylation and glycine, serine, and threonine metabolism. In addition, the MSTRG.15920.1-*REC8*-MSTRG.11860.2-*VWC2* pathway may regulate sperm motility. This study helped elucidate the molecular genetic mechanism of sperm motility in chicken.

Key words: *Gushi* chicken, RNA-seq, testis, sperm motility

INTRODUCTION

The breeding male occupies a pivotal position in the breeding system. Semen quality is an index of the breeding ability of roosters and affects the egg fertilization rate and even the production performance of the offspring. Low sperm motility is the main manifestation of low fertility in poultry production, and 80% of low fertility breeding males have low sperm motility (Hu et al., 2013).

Sperm motility is an indicator of semen quality (Bondarenko et al., 2019) and is measured by the percentage of sperm cells that move in a straight line during ejaculation. In mammals, spermatozoa have weak or no motility after exiting the varicocele; motility is acquired in the epididymis but remains quiescent (Vyklicka et al., 2020). Spermatozoa undergo several physiological and biochemical modifications in the male reproductive tract to gain fertilization competence (Zalazar et al., 2020). Poultry sperm viability is low, intermediate, and high in the testis, epididymis, and vas deferens, respectively (Ahammad et al., 2011). Chicken spermatozoa are immotile at $\geq 40°C$ and resume motility at 30°C, Motility is determined by Ga^{2+} homeostasis and the regulation of multiple enzymes, including myosin light chain kinase, protein kinase A, and phosphatases (Ashizawa et al., 2010; Nguyen, 2019).

Transcriptional gene regulation plays a key role in multiple physiological processes, including sperm motility (Song et al., 2019). For instance, *DNAH1* mutations in the testis of mice led to defects in sperm flagella, resulting in reduced sperm motility (Coutton et al., 2019). In Atlantic salmon, the inhibitor HC-056456 bound to CatSper channel and blocked Ca^{2+} influx, inhibiting sperm activation and fertilization (Lissabet et al., 2020). While the genetic molecular mechanisms underlying sperm motility have been studied in terrestrial mammals and marine animals, most studies on sperm motility in chickens focused on the effect of external factors and trace elements. For instance, the addition of trace elements such as zinc and selenium and organic matter such as flaxseed oil to the diet can improved sperm motility and sperm quality in poultry (Huang et al., 2019; Abbaspour et al., 2020). Sperm motility and viability were higher in geese maintained under artificial white light than in birds kept under blue and red light (Chang et al., 2016). However, improvements in poultry husbandry reduced the effects of external factors on sperm motility. Proteomic analysis has

shown that seminal plasma proteins adhesion G protein-coupled receptor and serine peptidase inhibitor Kazal-type 2 have a key role in maintaining sperm motility in chickens (Li et al., 2020).

This study performed RNA-Seq of the testes of sexually mature *Gushi* roosters with high and low sperm motility to identify differentially expressed (**DE**) RNAs involved in sperm motility. These results helped identify the factors affecting the reproductive performance of chickens.

MATERIALS AND METHODS

All animal experiments were performed in accordance with the regulations of the Chinese National Research Council (1994) and were approved by the Animal Care and Use Committee of Henan Agricultural University (Permit Number:11-0085).

Sample Collection

From 238 roosters, 79 healthy 28-wk-old *Gushi* roosters of similar weight were selected and these animals were kept in the same environment. Semen quality was assessed twice a week for 4 wk using a light microscope, and pH was measured using a pH test paper. At 32 wk of age, 3 animals with high sperm motility (H1, H2, and H3) and 3 with low sperm motility (L1, L2, and L3) were anesthetized with an intravenous injection of sodium pentobarbital (30 mg/kg) and euthanized by cervical dislocation. The right testis of each animal was excised, transferred to an RNase-free centrifuge tube containing tissue RNA preservation solution, and stored at −80°C for analysis.

RNA Library Preparation and Sequencing

Total RNA was extracted from the testes using TRIzol (Vazyme, Zhengzhou, China) and resuspended in RNase-free ddH2O. RNA degradation and contamination were detected using 1% agarose gels, and RNA integrity was assessed using an Agilent 2100 bioanalyzer (Agilent Technologies, CA). Total RNA (3 μg per sample) was used to construct each sequencing library. In this project, the mRNA with polyA structure in the total RNA was enriched by Oligo(dT) magnetic beads, and the RNA was broken to a fragment of about 300 bp in length by ion interruption. The first strand of cDNA was synthesized with 6-base random primers and reverse transcriptase using the RNA as template, and the second strand of cDNA was synthesized using the first strand of cDNA as template. After library construction, PCR amplification was used for library fragment enrichment, followed by library selection based on fragment size, which was 450 bp. Then, the libraries were quality checked by Agilent 2100 Bioanalyzer, and the total library concentration and effective library concentration were tested. The libraries containing different Index sequences (each sample with a different Index, and finally the downstream data of each sample according to the Index) were mixed proportionally according to the effective concentration of the library and the amount of data required for the library. The mixed libraries are uniformly diluted to 2 nM, and single-stranded libraries are formed by alkali denaturation. After RNA extraction, purification, and library construction, these libraries were sequenced using Next-Generation Sequencing (**NGS**) based on the Illumina sequencing platform with Paired-end (**PE**) sequencing.

Read Alignment and Assembly

Adapter sequences, primers, and reads with quality scores below 20 were removed using Cutadapt software, and paired-end reads were mapped to the chicken genome (GCF_000002315.6_GRCg6a_genomic.fna) using HISAT2 software. The number of aligned reads was counted using the HTSeq package for Python, and transcripts were classified as coding sequences, introns, intergenic regions, and UTR. Contigs were assembled into transcripts using Cufflinks version 2.2.1. Transcript levels were expressed as fragments per kilobase of exon per million fragments mapped (**FPKM**), and transcripts with FPKM >1 were considered differentially expressed.

Identification of lncRNAs

The eukaryotic transcriptome non−strand-specific library was used to obtain lncRNAs, and mapped reads were assembled using the Stringtie/Hisat2 pipeline. Transcripts with indeterminate strand orientation were removed, and lncRNAs were identified. The coding potential of predicted lncRNAs can determine whether new transcripts encode proteins.

Analysis of Differential Expression

The differential expression of mRNAs and lncRNAs was quantified with DESeq using log2 fold-change>|1.5| and false-discovery rate <0.05 as cut-off criteria. Samples were hierarchically clustered based on RNA expression levels using the hclust package in R. DE lncRNAs between roosters with high and low sperm motility were identified by two-way hierarchical clustering analysis using complete linkage Euclidean distances.

Prediction of Target Genes

Cis-regulatory elements located within 10 kbp upstream and downstream of lncRNAs were predicted using jPREdictor (http://bibiserv.techfak.uni-bielefeld.de/jpredictor), as described previously. Pearson correlation coefficients between DE lncRNAs and mRNAs were calculated to identify co-expressed lncRNA-mRNA pairs. The threshold was set to >0.5, and the FDR was set to <0.01.

Functional Enrichment Analysis

Gene Ontology (**GO**) enrichment analysis was performed using topGO, assuming that the expected number of target genes assigned to each GO term followed a hypergeometric distribution. Kyoto Encyclopedia of Genes and Genomes (**KEGG**) enrichment analyses were performed using g:Profiler (https://biit.cs.ut.ee/gprofiler/gost/). *P*-values of less than 0.05 were considered statistically significant.

Real-Time Quantitative Polymerase Chain Reaction

RNA was reverse transcribed into cDNA using the HiScript III RT SuperMix kit (Vazyme). Real-Time Quantitative Polymerase Chain Reaction (**RT-qPCR**) was performed using SYBR Green I on a LightCycler96 system (Roche Diagnostics, Zhengzhou, China). The transcription level of each target gene was normalized to the housekeeping gene *GAPDH* using the $2^{-\Delta\Delta Ct}$ method. The reaction mixture contained 5 μL of SYBR Green Mix, 3 μL of RNA-free water, 0.5 μL of each primer, and 1 μL of cDNA. Amplification conditions consisted of an initial denaturation step at 95°C for 5 min followed by 40 cycles at 95°C for 30 s, 60°C for 30 s, and 72°C for 30 s. The experiments included 6 biological replicates performed in triplicate. Primers are shown in Table 1.

Statistical Analyses

Data were analyzed by one-way analysis of variance followed by Duncan's multiple range test using SPSS version 23.0. *P*-values of less than 0.05 were considered statistically significant. Data are means ± standard errors and were plotted using GraphPad Prism version 7.0.

RESULTS

Assessment of Semen Quality

The ejaculate volume of 79 roosters was 0.37 ± 0.12 mL, pH was 7.70 ± 0.20, sperm motility was 0.51 ± 0.12, sperm viability was 0.76 ± 0.05, sperm density was 20.00 ± 460 million/mL, and sperm malformation rate was 0.13 ± 0.03. The median sperm motility was 0.52, and the lower and upper quartile was 0.42 and 0.61 (Figure 1A). The frequency distribution of sperm motility was normal (Figure 1B). Based on previous results, sperm motility below 0.42 and above 0.61 was considered low and high, respectively. Three animals with high sperm motility (0.74 ± 0.03) and 3 with low motility (0.24 ± 0.02) were selected for analysis of differential expression.

Quality of Transcriptome Data

To screen genes related to testicular development and sperm viability, 6 libraries (L1, L2, L3, H1, H2, H3)

Table 1. Gene primer sequences.

| Genes	Primer sequences	Login Number	Product length
GAPDH	F: GAACATCATCCCAGCGTCCA R: CGGCAGGTCAGGTCAACAAC	NM_204305	132
KCNK2	F: ATCCCAAATCGGCCACTCAG R: AGGTTTCATGAGGCTGCTCC	XM_004935320	229
DIO2	F: GCTTCAGATCTTGCCGGTCT R: TCTCCTCCAAGTTTGACCGC	NM_204114	195
HABP2	F: AGCACCCCTGGATGGTATCT R: TTAGCGCTCCACCACAGAAG	NM_001277379	243
ANO8	F: ACCTCAAAGACATGGAGCGG R: AGGAACTGCCGTGTGATGAG	XM_040653731	208
OMP	F: GGGAGGTGTGCTCAAGAGTG R: TAGACCAGGCTGCTCAATGC	XM_004938942	222
TPPP3	F: GCAAAGTCATCGACGGCAAA R: CGTTAATGGGCTCCTTCCCA	XM_015279191	207
KCNIP1	F: CAAGCTGTTCCGGCCTGTTA R: GCTAGCATCTCCGTGAGGAA	XM_040647085	204
CRYAB	F: CCTTCTTTCGGATGCCCAGT R: GCTCCTCGTGTTTCCCATGA	NM_205176	162
KIFC1	F: AACATCCGTGTGTTTTGCCG R: CGCGATCAAAGCTGAAGTCG	NM_001081698	152
MSTRG.15920.1	F: TGAAGGAGTGCGGTGTCTTC R: GGGGTTCCCAAAGCACCTT	——	157
HBBA	F: CTATCCCCACGGGAGCAAGA R: AGGTTCCCAAAGGACGCAAA	NM_205489	217
MSTRG.33244.1	F: CATGGCAACCTTCGAGGACT R: ATGGTCTCACTGCGTCTCAC	——	197
MSTRG.9747.1	F: GCACCAGGTGAACCCTTCAT R: AGGCTTTAACTGACCCAGGC	——	168
REC8	F: TTTGTCTGGATCTGTGCGCT R: GGTCCAATAAAAGAGCGCCG	XM_040655012.2	166
MSTRG.11860.2	F: GAGAAGTGGGATGGAGCCAC R: CAGATGAAGCCCAGCCTGAT	_ _ _ _ _	157
VWC2	F: TTTCGGGGGAAGACCTACC R: GTCAGTCTTCACCTCTCGGC	XM_046937859.1	228
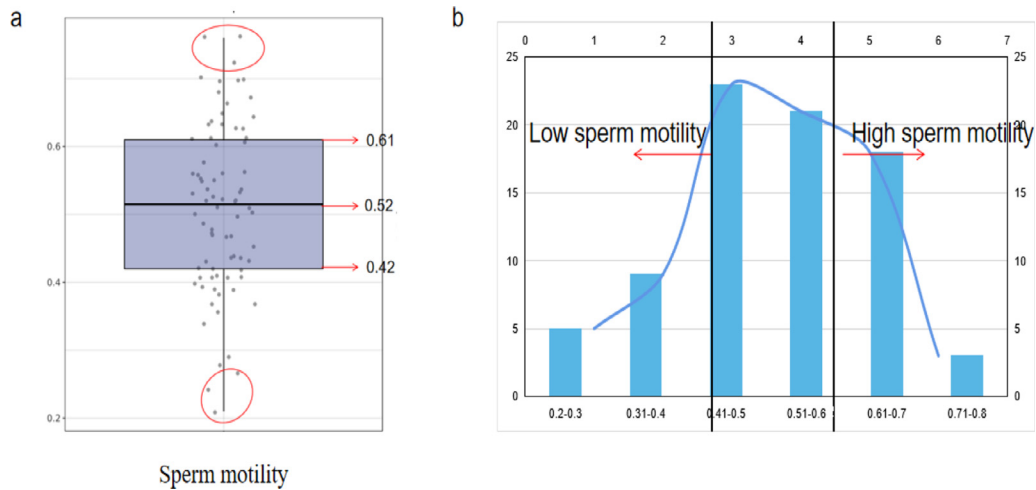
Figure 1. Sperm quality in Gushi chickens. (A) Sperm motility in 79 male chickens. The median sperm motility was 0.52, and the lower and upper quartile was 0.42 and 0.61. (B) Frequency distribution of sperm motility in animals with low sperm motility (below the lower quartile, N = 3) and high sperm motility (above the upper quartile, N = 3).

were paired-end sequenced on an Illumina platform. The number of high-quality reads in these libraries was 49673570, 45968990, 43805848, 41691346, 46183652, and 39461786, respectively. The percentage of mapped and unique reads was >92% and >96%.

Analysis of DE mRNAs in Testicular Tissue

DE mRNAs from both groups were counted. A total of 16,837 mRNAs were identified, of which 191 and 195 were specifically expressed in the low and high sperm motility groups, respectively (Figure 2A). A total of 140 mRNAs were DE, of which 73 were upregulated and 67 were downregulated (Figure 2B). Several genes were associated with spermatogenesis and sperm motility, including *KIFC1, REC8* and *DIO2* (Table 2). DE

mRNAs were clustered into 2 major groups based on fold-change (Figure 2C).

GO and KEGG Enrichment Analyses

Functional enrichment analysis was performed to identify pathways associated with sperm viability. mRNAs were enriched in genes encoding G protein-coupled receptors (**GABBR2**), heat-shock proteins (*CRYAB* and *HSPB2*), and alpha-B crystallin (**CRYAB**) (Table 3). KEGG analysis showed that genes associated with oxidative phosphorylation (*NDUFAB1, COX5A* [downregulated] and *MAOB* [upregulated]) and glycine, serine, and threonine metabolism could be involved in the regulation of sperm motility (Table 4; Huang et al., 2018; Nguyen et al., 2019).
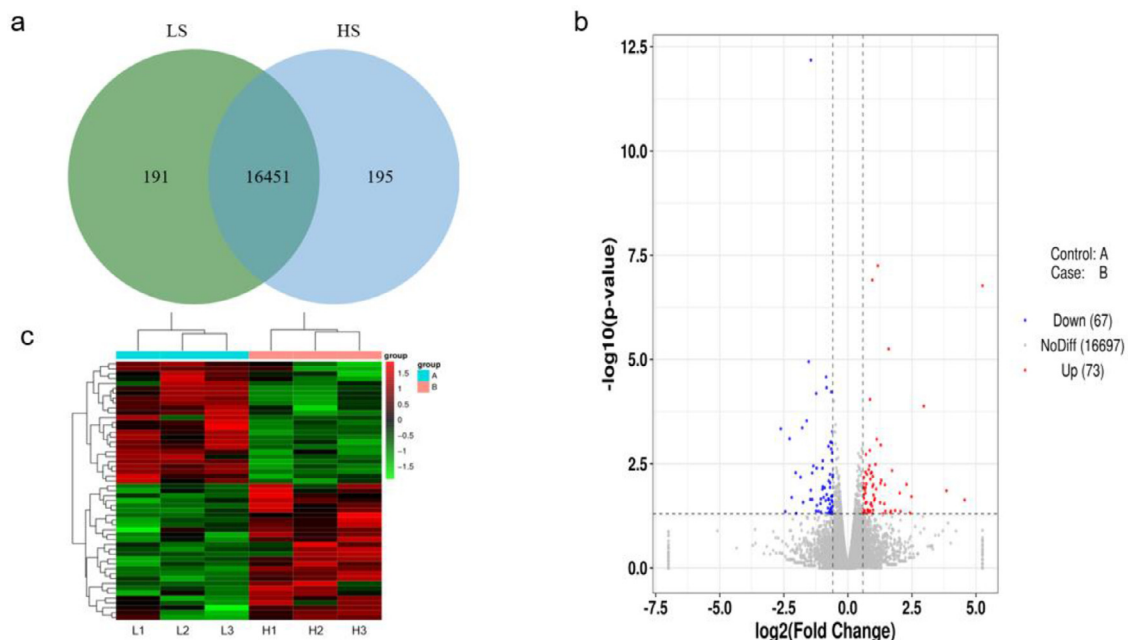

Figure 2. Analysis of differentially expressed mRNAs between male chickens with low sperm motility (LS) and high sperm motility (HS). (A) Differentially expressed genes (DEGs). A total of 191 and 195 DEGs were specifically expressed in the LS and HS, respectively. (B) Volcano plot of differentially expressed mRNAs. (C) Heatmap of differentially expressed mRNAs; 73 genes were upregulated and 67 were downregulated.

Table 2. Differential genes related to spermatogenesis and sperm motility.

Gene	Expression status	Function
KIFC1	down	Participates in mitosis of spermatogonia, meiosis of spermatocytes and acrosome formation during spermatogenesis (Hao et al., 2019; Gao et al., 2019).
REC8	up	Meiosis affecting spermatogenesis (Xu et al., 2005; Lin et al., 2020).
KCNK2	up	K(2P) channels regulate processes such as germ cell maturation, fertilization and development (Hur et al., 2009).
UXT	up	Essential for spermatogenesis and fertility in germ cells (Schafler et al., 2018; Thomas et al., 2020).
SLC26A7	up	Regulation of testicular anions, thus regulating sperm motility (Kujala et al., 2007).
DIO2	up	Acts in testicular cells, thereby affecting steroidogenesis, sperm production and male fertility (Hernandez 2018).
C1QTNF3	down	Increasing C1q/TNF-related protein 3 improves sperm count and sperm motility (Mu et al., 2018).

Validation of RNA-Seq results

RNA-Seq data were validated by RT-qPCR. Nine DE genes—*KCNK2, DIO2, HABP2, ANO8, CRYAB, KIFC1, OMP, TPPP3,* and *KCNIP1*—were selected at random (Table 5). PCR results showed that *KCNK2, DIO2, HABP2, ANO8*, and *CRYAB* were upregulated,

whereas *KIFC1, OMP, TPPP3*, and *KCNIP1* were downregulated in the group with high sperm motility, consistent with RNA-Seq results (Figure 3; Li et al., 2019).

Identification of lncRNAs

LncRNAs were identified using PLEK, CNCI, and PfamScan (Kong et al., 2007), and 7,830 lncRNAs were selected for subsequent analysis. To assess the effect of mRNA levels on sperm viability, DE lncRNAs between the 2 study groups were integrated. mRNA sequences were longer than lncRNAs (Figure 4A). The number of transcripts (Figure 4B). Most lncRNAs contained 2 or 3 exons, whereas most mRNAs had more than 10 exons (Figure 4C), in line with previous results (Li et al., 2020). A total of 7,400 lncRNAs were co-expressed in the high and low sperm viability groups; of these, 227 and 202 were specifically expressed in the low sperm viability and high sperm viability groups, respectively (Figure 4D). A total of 103 lncRNAs were DE: 56 were downregulated (31 in the low sperm viability group), and 47 were upregulated (25 in the high sperm viability group; Figure 4E). LncRNAs were clustered into 2 major groups based on fold-change (Figure 4F).

Analysis of DE lncRNAs

To further investigate how lncRNAs and their target genes regulate sperm motility, functional enrichment

Table 3. The most highly enriched GO terms.

Category	GO.ID	Term	Total	DEG	*P*-value	Up_Gene	Down_Gene
CC	GO:0038039	G protein-coupled receptor heterodimeric complex	1	1	0.0062	-	*GABBR2*
CC	GO:0005581	collagen trimer	31	2	0.016	*C1QL1*	*C1QTNF3*
CC	GO:0005576	extracellular region	774	10	0.019	*BMP3, C1QL1, FGF13, LOC100858942, OVALX*	*C1QTNF3, CHADL, FBLN1, FRZB, HBBA*
CC	GO:0031838	haptoglobin-hemoglobin complex	5	1	0.031	-	*HBBA*
CC	GO:0038037	G protein-coupled receptor dimeric complex	5	1	0.031	-	*GABBR2*
CC	GO:0097648	G protein-coupled receptor complex	5	1	0.031	-	*GABBR2*
MF	GO:0005212	structural constituent of eye lens	14	1	0.0032	*CRYAB, HSPB2*	-
MF	GO:0000036	acyl carrier activity	1	1	0.0061	-	*NDUFAB1*
MF	GO:0030492	hemoglobin binding	1	1	0.0061	-	*HBBA*
MF	GO:0044620	ACP phosphopantetheine attachment site binding	1	1	0.0061	-	*NDUFAB1*
MF	GO:0051192	prosthetic group binding	1	1	0.0061	-	*NDUFAB1*
MF	GO:0070579	methylcytosine dioxygenase activity	1	2	0.0061	-	*TET2*
BP	GO:0006211	5-methylcytosine catabolic process	1	1	0.0055	-	*TET2*
BP	GO:0019857	5-methylcytosine metabolic process	1	1	0.0055	-	*TET2*
BP	GO:0021577	hindbrain structural organization	1	1	0.0055	-	*DAB1*
BP	GO:0021589	cerebellum structural organization	1	1	0.0055	-	*DAB1*
BP	GO:0021942	radial glia guided migration of Purkinje cell	1	1	0.0055	-	*DAB1*
BP	GO:1905907	negative regulation of amyloid fibril formation	1	1	0.0055	*CRYAB*	-

CC stands for "cellular component", MF stands for "molecular function" and BP stands for "biological process".

Table 4. The top 20 KEGG pathways significantly enriched to differential genes.

Pathway ID	Pathway	total_number	DEG_number	P-value	Up_gene	Down_gene
gga00340	Histidine metabolism	20	2	0.0075	*MAOB*	*CNDP1*
gga04060	Cytokine-cytokine receptor interaction	202	5	0.011	*IL1R2, TNFRSF8, IL18R1, BMP3*	*IL1RL2*
gga04672	Intestinal immune network for IgA production	38	2	0.026	*BLB2*	*MADCAM1*
gga00330	Arginine and proline metabolism	42	2	0.031	*MAOB*	*CNDP1*
gga04514	Cell adhesion molecules (CAMs)	125	3	0.049	*CD2, BLB2*	*MADCAM1*
gga00360	Phenylalanine metabolism	13	1	0.082	*MAOB*	-
gga00770	Pantothenate and CoA biosynthesis	14	1	0.088	*VNN1*	-
gga00532	Glycosaminoglycan biosynthesis - chondroitin sulfate / dermatan sulfate	19	1	0.12	-	*CHST12*
gga00040	Pentose and glucuronate interconversions	22	1	0.14	-	*XYLB*
gga00563	Glycosylphosphatidylinositol (GPI)-anchor biosynthesis	22	1	0.14	-	*PIGP*
gga04744	Phototransduction	23	1	0.14	-	*SAG*
gga00190	Oxidative phosphorylation	103	2	0.15	-	*NDUFAB1, COX5A*
gga00410	beta-Alanine metabolism	25	1	0.15	-	*CNDP1*
gga00350	Tyrosine metabolism	33	1	0.20	*MAOB*	-
gga00982	Drug metabolism - cytochrome P450	35	1	0.21	*MAOB*	-
gga00260	Glycine, serine and threonine metabolism	36	1	0.21	*MAOB*	-
gga00380	Tryptophan metabolism	37	1	0.22	*MAOB*	-
gga04260	Cardiac muscle contraction	56	1	0.31	-	*COX5A*
gga00561	Glycerolipid metabolism	60	1	0.33	-	*DGKI*
gga04070	Phosphatidylinositol signaling system	89	1	0.45	-	*DGKI*

analysis was performed on 15,895 genes regulated in cis and 3,000 genes regulated in trans. DE genes were implicated in growth and development, reproduction, immunity, and metabolism (Figure 5A) and were significantly enriched in mTOR signaling, VEGF signaling, phosphatidylinositol signaling, RNA transport, and aminoacyl-tRNA biosynthesis (Figure 5B).

LncRNA-mRNA Interaction Network

The interactions between lncRNAs and mRNAs were analyzed using the igraph package in R (Figure 6). Seven cis-regulated genes interacted with 7 lncRNAs. The genes *HBBA, TET2,* and *SH3TC1* were downregulated, and *C1QL1, LOC112530336, LOC100858942,*

Table 5. Information on the expression amount, location, and length of some of the differential genes in the sequenced samples.

| ID	baseMean_A	baseMean_B	foldChange(B/A)(B/A)	P-value	Chromosome	Start site	End site	Length
C1QTNF3	80.44	40.42	0.50	0.0040	NC_006127.5	10370845	10387499	2927
OMP	23.62	5.75	0.24	0.0052	NC_006088.5	1.95E+08	1.95E+08	5634
GABBR2	127.19	81.34	0.64	0.019	NC_006089.5	87910767	88370525	5283
HBBA	38.12	18.18	0.48	0.026	NC_006088.5	1.97E+08	1.97E+08	618
COX5A	138.19	58.48	0.42	0.043	NC_006097.5	2847964	2852187	639
KCNIP1	95.01	32.91	0.35	1.14E-05	NC_006100.5	4271439	4564776	3017
TPPP3	2,375.80	1,317.92	0.55	2.64E-05	NC_006088.5	1221961	1224452	1188
ZNF692	398.77	223.88	0.56	4.74E-05	NC_006103.5	2446991	2453265	1686
ATP13A4	356.24	116.87	0.33	0.00029	NC_006096.5	13237177	13270734	4810
KIFC1	1,008.47	293.20	0.29	0.00044	NC_006103.5	2439128	2443841	2181
SH3TC1	158.32	25.78	0.16	0.00045	NC_006091.5	80795858	80825419	4861
NDUFAB1	508.75	312.58	0.61	0.029	NC_006101.5	7277376	7279310	682
DAB1	30.53	13.79	0.45	0.044	NC_006095.5	26199586	26572397	6174
ANO8	125.74	282.97	2.25	5.69E-08	NC_006115.5	3514382	3523356	3776
REC8	258.06	499.61	1.94	1.25E-07	NW_020110164.1	1747896	1751916	1417
CRYAB	63.29	190.53	3.01	5.61E-06	NC_006111.5	6242317	6246235	1219
SLC6A11	132.42	240.89	1.82	9.06E-05	NC_006099.5	4459519	4545606	5563
VWC2	135.21	220.34	1.63	0.0019	NC_006089.5	80493366	80551992	1889
MAOB	80.73	135.18	1.67	0.0057	NC_006088.5	1.13E+08	1.13E+08	6096
BMP3	47.97	118.42	2.47	0.0079	NC_006091.5	45450067	45474587	5383
MROH7L4	74.68	122.93	1.65	0.0096	NC_006127.5	67440358	67443254	1070
SLC26A7	109.64	167.81	1.53	0.013	NC_006089.5	1.25E+08	1.25E+08	10553
PKP3	79.43	158.77	2.00	0.018	NC_006092.5	1782404	1792449	3159
UXT	58.32	119.15	2.04	0.024	NC_028739.2	337454	342057	763
DIO2	12.67	30.35	2.40	0.027	NC_006092.5	40752222	40769122	6090
HABP2	8.183	21.14	2.58	0.050	NC_006093.5	28347735	28407872	2242
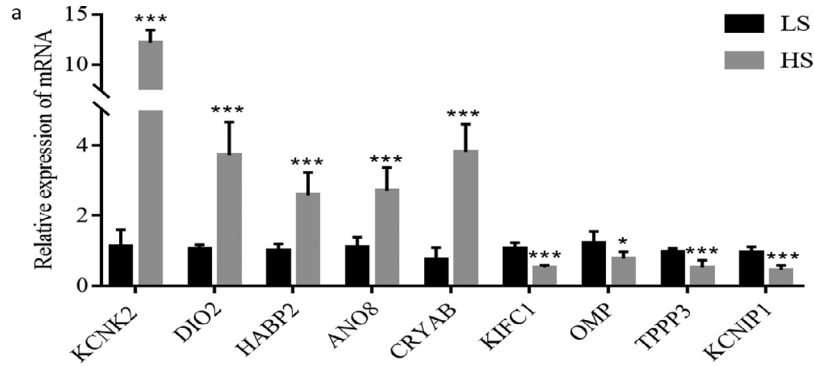
Figure 3. Concordance between RNA-Seq and RT-qPCR results. (A) RT-qPCR analysis of relative gene expression in male chickens with low sperm motility (LS) and high sperm motility (HS). (B) RNA-Seq analysis of differentially expressed genes in the LS and HS (*$P \leq 0.05$, **$P \leq 0.01$, ***$P \leq 0.001$).

and *LOC112531346* were upregulated. Thirteen trans-regulated genes interacted with 12 lncRNAs. The genes *LRRC74A, BORCS6, TPPP3, TEF, LOC112530178, CHST12,* and *ZNF692* were downregulated, and *LOC101749307, LOC107054355, MROH7L4, CRYAB, REC8,* and *VWC2* were upregulated. *REC8* inhibited MSTRG.15920.1 and MSTRG.11860.2, whereas *VWC2* inhibited MSTRG.11860.2. *REC8* affects sperm meiosis, and *VWC2* is a bone morphogenetic protein antagonist (Almehmadi et al., 2018). *BMP4* promotes the formation of primordial germ cells in chickens (Zuo et al., 2019).

DISCUSSION

Chicken is an economically important livestock product. The reproductive performance of breeding males has a significant economic impact on the poultry industry, and semen quality is an indicator of the reproductive performance of males (Bhave et al., 2020; Tesfay et al., 2020). Nonetheless, international standards for evaluating chicken semen quality are currently unavailable, and the present study intended to fill this gap. Sperm viability below 0.42 and above 0.61 was considered low and high, respectively. These data can serve as a basis for assessing the semen quality of breeding hens.
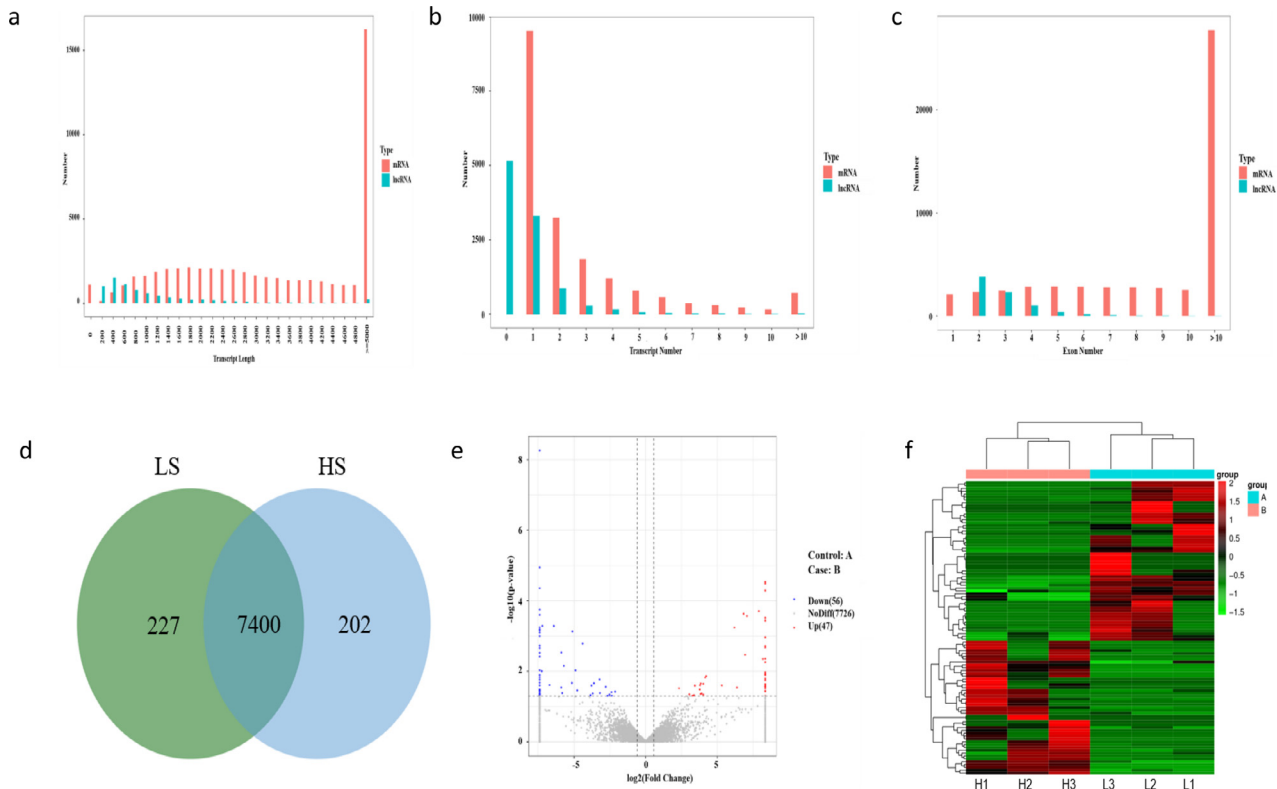

Figure 4. Analysis of differentially expressed lncRNAs between male chickens with low sperm motility (LS) and high sperm motility (HS). (A) Length of lncRNAs and mRNAs. (B) Number of lncRNA and mRNA transcripts. (C) Number of exons in lncRNAs and mRNAs. (d) Number of lncRNAs in the LS and HS. A total of 227 and 202 lncRNAs were specifically expressed in the LS and HS, respectively. (E) Differentially expressed lncRNAs: 47 lncRNAs were upregulated and 56 were downregulated. (F) Differentially expressed lncRNAs were grouped into two clusters according to fold-change.
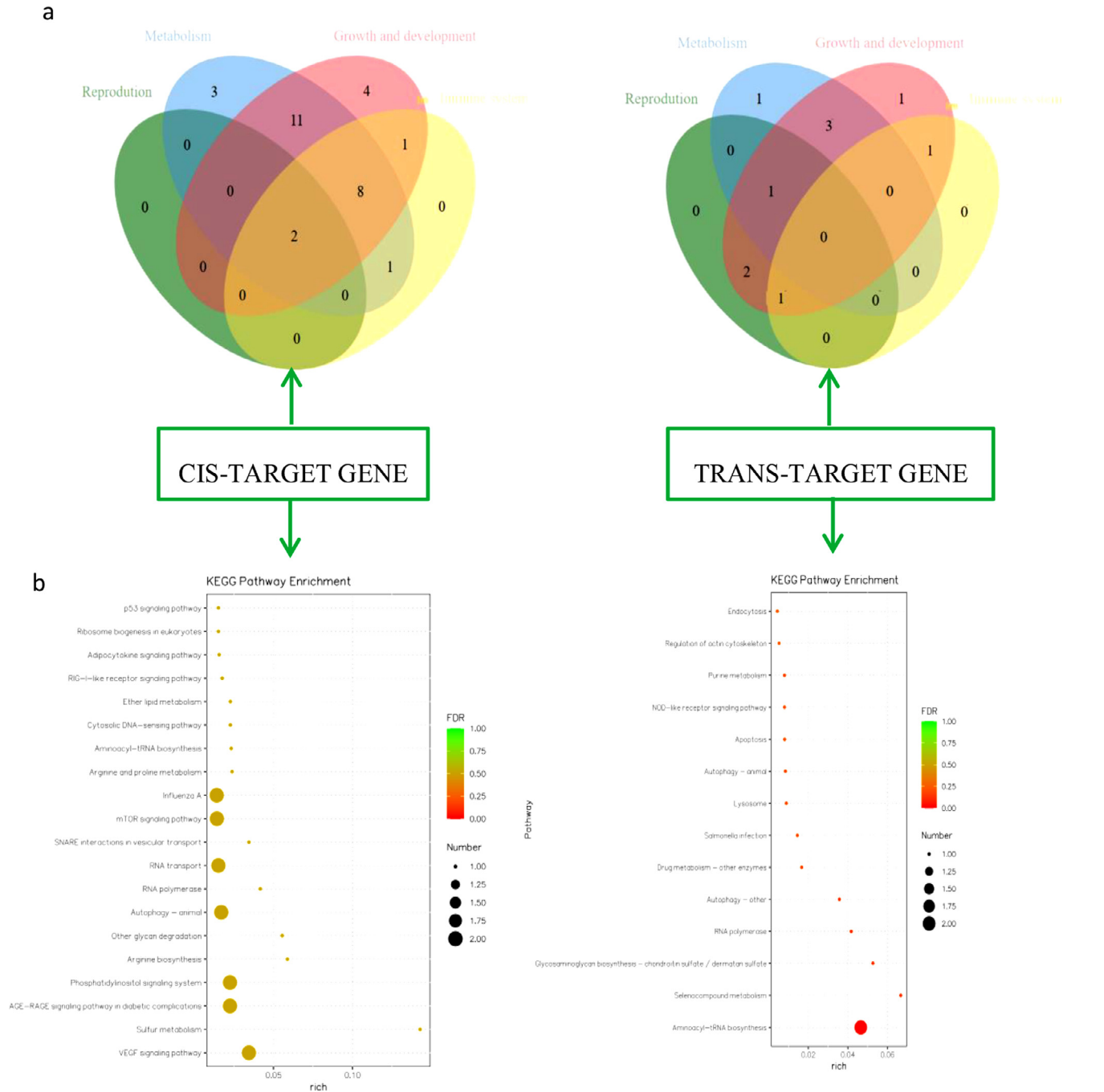
a

CIS-TARGET GENE

TRANS-TARGET GENE

b

Figure 5. Functional annotation and enrichment analysis of cis-and transregulated genes. (A) Functional classification. (B) Pathway enrichment analysis. Gene ontology (GO) classification revealed that most genes were involved in growth and development, reproduction, immunity, and metabolism.

Avian spermatogenesis is a complex process regulated by the endocrine hypothalamic-pituitary-testicular axis (Xu et al., 2017; Wang et al., 2019). RNA-Seq of testes from animals with high and low sperm viability was performed to identify RNAs affecting spermatogenesis and sperm motility. Several genes were DE between these groups, including *KCNK2* and *KIFC1*. *KIFC1*, a member of the kinesin 14 family, was expressed in human spermatocytes, and the knockdown of this gene inhibited testicular cancer cell division (Xiao et al., 2017; Teng et al., 2019). *KIFC1* may be involved in mitosis in spermatogonia, meiosis in spermatocytes, and acrosome formation in spermatogenesis in Japanese shrimp, and the

inhibition of *KIFC1* expression causes apoptosis in spermatocytes (Hao et al., 2019). *KIFC1* is essential for spermatogenesis in Phascolosoma esculenta, red swamp crayfish (*Procambarus clarkii*), Chinese mitten crab (*Eriocheir sinensis*), and Portunus trituberculatus (Ma et al., 2017; Gao et al., 2019; Wei et al., 2019). *KCNK2* is a member of the K2P channel family and is expressed in bovine ovaries, testes, oocytes, and spermatozoa (Hur et al., 2009). Potassium channels regulate various physiological processes in mammalian germ cells, including sperm motility (Winston et al., 2004; Yang et al., 2004).

The molecular mechanisms and signal transduction pathways controlling sperm motility include intracellular
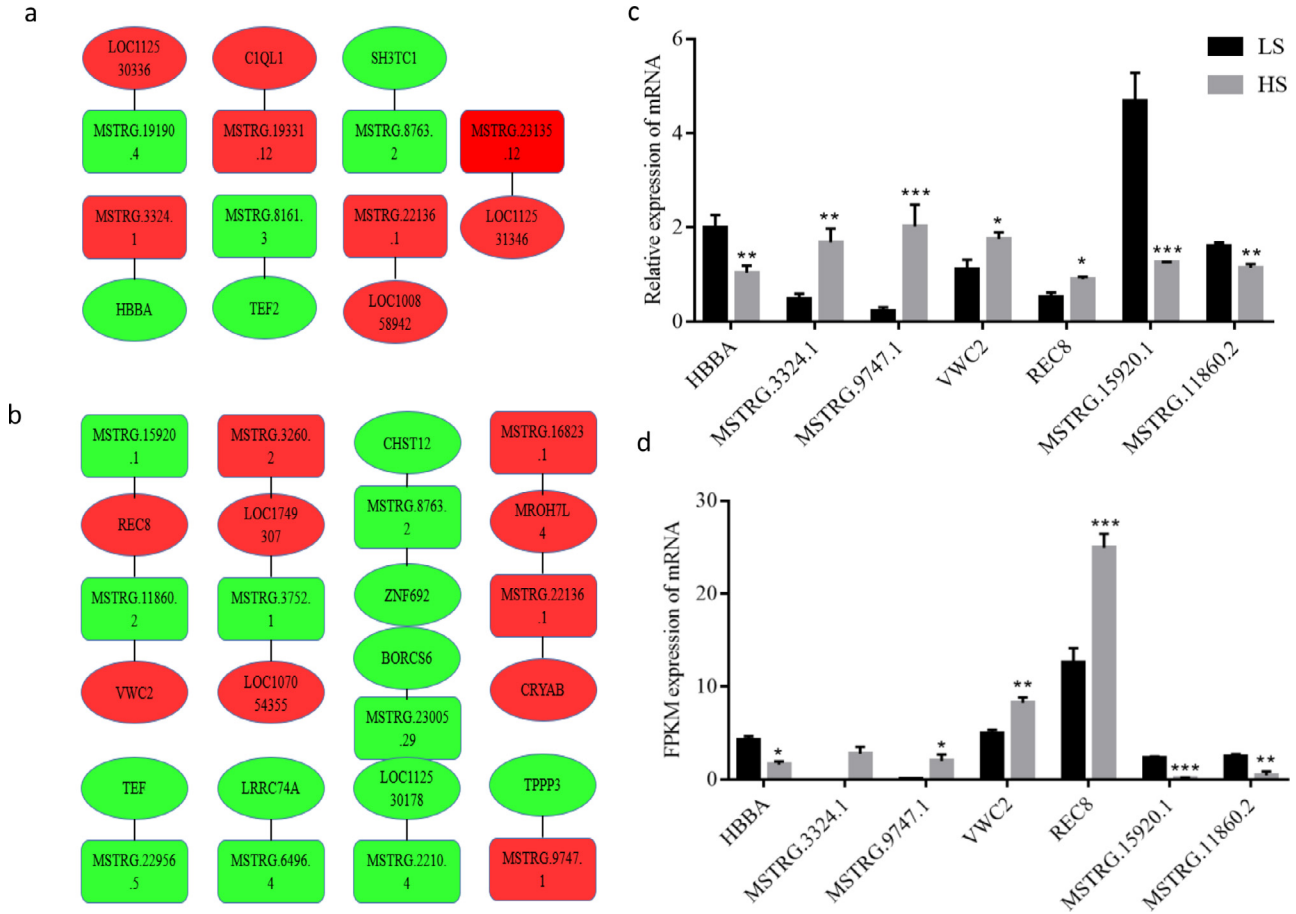
Figure 6. LncRNA-mRNA interaction network and concordance between RT-qPCR and RNA-Seq results. (A) Interaction between lncRNAs and cis-regulated genes. (B) Interaction between lncRNAs and transregulated genes. Rectangles represent lncRNAs, ellipses represent target genes, and green indicates downregulation. (C and D) RT-qPCR and RNA-Seq analysis of the relative expression of mRNAs and lncRNAs in male chickens with low sperm motility (LS) or high sperm motility (HS).

calcium levels, lipid transfer in the sperm plasma membrane, phospholipid remodeling, and protein phosphorylation (Ashizawa et al., 1994; Han et al., 2007). Moreover, protein kinase A (**PKA**) and phosphatases control sperm motility (Priyadarshana et al., 2020). Mitochondria are the energy-producing units of the testis that support the energy expenditure of sperm to obtain power, and if they are damaged sperm viability must be affected. Functional enrichment analysis showed that pathways associated with oxidative phosphorylation and glycine, serine, and threonine metabolism affected sperm viability, and *NDU-FAB1* (Hou et al., 2019), *COX5A* (Xiyang et al., 2020), and *MAOB* (Raghavan et al., 2020) affect mitochondrial function. Our analysis showed that DE genes were enriched in processes related to reproduction and immunity. Immune cells protect germ cells against pathogens, and testicular macrophages promote spermatogenesis (Bhushan et al., 2020). The mTOR signaling pathway has an important role in spermatogonial stem cell proliferation and differentiation, blood-testis barrier remodeling, and spermatogenesis of Sertoli cells (Moreira et al., 2019).

Our results showed that lncRNAs regulated several genes, including *REC8, CRYAB*, and *TPPP3*. MSTRG.15920.1 upregulated the gene adhesion element *REC8*, which upregulated the lncRNA

MSTRG.11860.2 and the mRNA *VWC2. REC8* is expressed in mouse spermatocytes and oocytes (Lee et al., 2002 2003b; Rong et al., 2016) and has a key role in spermatogenesis and oogenesis (Xu et al., 2005; Lin et al., 2020). The cysteine junction protein *VWC2* increases bone formation through an antagonistic effect on BMP signaling (Almehmadi et al., 2018). The lncRNA MSTRG.22136.1 regulated the alpha-B crystallin gene *CRYAB. CRYAB* is involved in eye and heart diseases and cancers (Tang et al., 2018; Zhang et al., 2019; Ruan et al., 2020). In addition, *CRYAB* regulates apoptosis, inflammation, and oxidative stress. *CRYAB* was significantly upregulated in the testis of animals with high sperm motility, suggesting that this gene regulates sperm viability. MSTRG.9747.1 upregulated the tubulin polymerization-promoting protein family member 3 gene (*TPPP3*). *TPPP3* inhibition induces apoptosis in human endometrial stromal cells and reduces mitochondrial membrane potential, resulting in embryonic metaphase (Shukla et al., 2019). Moreover, the knockdown of *TPPP3* inhibits the proliferation, migration, and invasion ability of human rectal cancer cells and induces apoptosis in vitro (Ye et al., 2017). The interaction of these target genes may affect sperm motility.

CONCLUSIONS

RNA-Seq analysis identified differentially expressed mRNAs and lncRNAs in the testicular tissue of *Gushi* roosters. Several genes were involved in sperm motility, including *KIFC1* and *REC8*. The MSTRG.15920.1-*REC8*-MSTRG.11860.2-*VWC2* pathway and the lncRNA MSTRG.15920.1 affected sperm motility by regulating *REC8*. This study helped elucidate the molecular mechanisms of sperm motility in chicken.

ACKNOWLEDGMENTS

DISCLOSURES

The manuscript has been read and approved by all the named authors and there is no conflict of interest between us. We have given due consideration to the protection of intellectual property rights in relation to this work and there are no impediments to publication, including timing of publication, etc. We further confirm that any aspect of the experimental animal work involved in this manuscript was conducted with the ethical approval of all relevant institutions. We understand that the corresponding author is the sole point of contact for the editorial process (including the editorial manager and direct communication with the office). He/she is responsible for communicating progress with other authors, revision submissions and final approval proofreading.

SUPPLEMENTARY MATERIALS

Supplementary material associated with this article can be found, in the online version, at doi:10.1016/j.psj.2022.102183.

REFERENCES

Abbaspour, B., S. D. Sharifi, S. Ghazanfari, A. Mohammadi-Sangcheshmeh, and S. Honarbakhsh. 2020. Effect of dietary supplementation of whole flaxseed on sperm traits and sperm fatty acid profile in aged broiler breeder roosters. Reprod. Domest. Anim. 55:594–603.

Ahammad, M. U., C. Nishino, H. Tatemoto, N. Okura, Y. Kawamoto, S. Okamoto, and T. Nakada. 2011. Maturational changes in motility, acrosomal proteolytic activity, and penetrability of the inner perivitelline layer of fowl sperm, during their passage through the male genital tract. Theriogenology 76:1100–1109.

Almehmadi, A., Y. Ohyama, M. Kaku, A. Alamoudi, D. Husein, M. Katafuchi, Y. Mishina, and Y. Mochida. 2018. VWC2 increases bone formation through inhibiting activin signaling. Calcif. Tissue Int. 103:663–674.

Ashizawa, K., N. Kawaji, S. Nakamura, D. Nagase, H. Tatemoto, S. Katayama, K. Narumi, and Y. Tsuzuki. 2010. Temperature-dependent regulation of sperm motility of Ijima's copper pheasants (Syrmaticus soemmerringii ijimae), one of 'near threatened' species. Anim. Reprod. Sci. 121:181–187.

Ashizawa, K., H. Tomonaga, and Y. Tsuzuki. 1994. Regulation of flagellar motility of fowl spermatozoa: evidence for the involvement of intracellular free Ca2+ and calmodulin. J. Reprod. Fertil. 101:265–272.

Bhave, K., T. P. J. Koilpillai, V. Ragothaman, S. Sontakke, G. Joshi, and V. Ducrocq. 2020. Semen production and semen quality of indigenous buffalo breeds under hot semiarid climatic conditions in India. Trop. Anim. Health Prod. 52:2529–2539.

Bhushan, S., M. S. Theas, V. A. Guazzone, P. Jacobo, M. Wang, M. Fijak, A. Meinhardt, and L. Lustig. 2020. Immune cell subtypes and their function in the testis. Front. Immunol. 11:583304.

Bondarenko, V., and J. Cosson. 2019. Structure and beating behavior of the sperm motility apparatus in aquatic animals. Theriogenology 135:152–163.

Chang, S. C., Z. X. Zhuang, M. J. Lin, C. Y. Cheng, T. Y. Lin, Y. S. Jea, and S. Y. Huang. 2016. Effects of monochromatic light sources on sex hormone levels in serum and on semen quality of ganders. Anim. Reprod. Sci. 167:96–102.

Coutton, C., G. Martinez, Z. E. Kherraf, A. Amiri-Yekta, M. Boguenet, A. Saut, X. He, F. Zhang, M. Cristou-Kent, J. Escoffier, M. Bidart, V. Satre, B. Conne, S. Fourati Ben Mustapha, L. Halouani, O. Marrakchi, M. Makni, H. Latrous, M. Kharouf, K. Pernet-Gallay, M. Bonhivers, S. Hennebicq, N. Rives, E. Dulioust, A. Touré, H. Gourabi, Y. Cao, R. Zouari, S. H. Hosseini, S. Nef, N. Thierry-Mieg, C. Arnoult, and P. F. Ray. 2019. Bi-allelic mutations in ARMC2 lead to severe astheno-teratozoospermia due to sperm flagellum malformations in humans and mice. Am. J. Hum. Genet. 104:331–340.

Gao, X. M., D. L. Mu, C. C. Hou, J. Q. Zhu, S. Jin, and C. L. Wang. 2019. Expression and putative functions of KIFC1 for nuclear reshaping and midpiece formation during spermiogenesis of Phascolosoma esculenta. Gene 683:169–183.

Han, Y., C. J. Haines, and H. L. Feng. 2007. Role(s) of the serine/threonine protein phosphatase 1 on mammalian sperm motility. Arch. Androl. 53:169–177.

Hao, S. L., and W. X. Yang. 2019. KIFC1 is essential for normal spermatogenesis and its depletion results in early germ cell apoptosis in the Kuruma shrimp, Penaeus (Marsupenaeus) japonicus. Aging (Albany NY) 11:12773–12792.

Hernandez, A. 2018. Thyroid hormone role and economy in the developing testis. Vitam. Horm. 106:473–500.

Hou, T., R. Zhang, C. Jian, W. Ding, Y. Wang, S. Ling, Q. Ma, X. Hu, H. Cheng, and X. Wang. 2019. NDUFAB1 confers cardio-protection by enhancing mitochondrial bioenergetics through coordination of respiratory complex and supercomplex assembly. Cell Res. 29:754–766.

Hu, J., J. L. Chen, J. Wen, G. P. Zhao, M. Q. Zheng, R. R. Liu, W. P. Liu, L. H. Zhao, G. F. Liu, and Z. W. Wang. 2013. Estimation of the genetic parameters of semen quality in Beijing-You chickens. Poult. Sci. 92:2606–2612.

Huang, L., X. Li, W. Wang, L. Yang, and Y. Zhu. 2019. The role of zinc in poultry breeder and hen nutrition: an update. Biol. Trace Elem. Res. 192:308–318.

Huang, S., S. Cao, T. Zhou, L. Kong, and G. Liang. 2018. 4-tert-octylphenol injures motility and viability of human sperm by affecting cAMP-PKA/PKC-tyrosine phosphorylation signals. Environ. Toxicol. Pharmacol. 62:234–243.

Hur, C. G., C. Choe, G. T. Kim, S. K. Cho, J. Y. Park, S. G. Hong, J. Han, and D. Kang. 2009. Expression and localization of two-pore domain K(+) channels in bovine germ cells. Reproduction 137:237–244.

Kong, L., Y. Zhang, Z. Q. Ye, X. Q. Liu, S. Q. Zhao, L. Wei, and G. Gao. 2007. CPC: assess the protein-coding potential of transcripts using sequence features and support vector machine. Nucleic. Acids. Res. 35:W345–W349.

Kujala, M., S. Hihnala, J. Tienari, K. Kaunisto, J. Hästbacka, C. Holmberg, J. Kere, and P. Höglund. 2007. Expression of ion transport-associated proteins in human efferent and epididymal ducts. Reproduction 133:775–784.

Lee, J., T. Iwai, T. Yokota, and M. Yamashita. 2003. Temporally and spatially selective loss of Rec8 protein from meiotic chromosomes during mammalian meiosis. J. Cell Sci. 116:2781–2790.

Lee, J., T. Yokota, and M. Yamashita. 2002. Analyses of mRNA expression patterns of cohesin subunits Rad21 and Rec8 in mice:

germ cell-specific expression of rec8 mRNA in both male and female mice. Zoolog. Sci. 19:539–544.

Li, M., Z. Xie, Z. Cai, F. Su, G. Zheng, J. Li, S. Wang, S. Cen, W. Liu, S. Tang, G. Ye, Z. Li, R. Mi, Y. Pan, P. Wang, Y. Wu, and H. Shen. 2019. lncRNA-mRNA expression profiles and functional networks of mesenchymal stromal cells involved in monocyte regulation. Stem Cell. Res. Ther. 10:207.

Li, T., B. Chen, P. Yang, D. Wang, B. Du, and L. Kang. 2020. Long non-coding RNA derived from lncRNA-mRNA co-expression networks modulates the locust phase change. Genomics Proteomics Bioinform. 18:664–678.

Li, Y., Y. Sun, A. Ni, L. Shi, P. Wang, A. M. Isa, P. Ge, L. Jiang, J. Fan, H. Ma, G. Yang, and J. Chen. 2020. Seminal plasma proteome as an indicator of sperm dysfunction and low sperm motility in chickens. Mol. Cell. Proteomics 19:1035–1046.

Lin, F., F. Tong, Q. He, S. Xiao, X. Liu, H. Yang, Y. Guo, Q. Wang, and H. Zhao. 2020. In vitro effects of androgen on testicular development by the AR-foxl3-rec8/fbxo47 axis in orange-spotted grouper (Epinephelus coioides). Gen. Comp. Endocrinol. 292:113435.

Lissabet, J. F. B., L. Herrera Belén, M. Lee-Estevez, J. Risopatrón, I. Valdebenito, E. Figueroa, and J. G. Farías. 2020. The CatSper channel is present and plays a key role in sperm motility of the Atlantic salmon (Salmo salar. Comp. Biochem. Physiol. A Mol. Integr. Physiol. 241:110634.

Ma, D. D., L. Bi, and W. X. Yang. 2017. KIFC1 is essential for acrosome formation and nuclear shaping during spermiogenesis in the lobster Procambarus clarkii. Oncotarget 8:36082–36098.

Moreira, B. P., P. F. Oliveira, and M. G. Alves. 2019. Molecular mechanisms controlled by mTOR in male reproductive system. Int. J. Mol. Sci. 20:1633.

Mu, Y., T. L. Yin, L. Yin, X. Hu, and J. Yang. 2018. CTRP3 attenuates high-fat diet-induced male reproductive dysfunction in mice. Clin. Sci. (Lond.) 132:883–899.

Nguyen, T. M. D. 2019. Main signaling pathways involved in the control of fowl sperm motility. Poult. Sci. 98:1528–1538.

Nguyen, T. M. D., I. Grasseau, and E. Blesbois. 2019. New insights in the AMPK regulation in chicken spermatozoa: role of direct AMPK activator and relationship between AMPK and PKA pathways. Theriogenology 140:1–7.

Priyadarshana, C., R. Setiawan, A. Tajima, and A. Asano. 2020. Src family kinases-mediated negative regulation of sperm acrosome reaction in chickens (Gallus gallus domesticus. PLoS One 15: e0241181.

Raghavan, S., D. S. Baskin, and M. A. Sharpe. 2020. MP-Pt(IV): A MAOB-sensitive mitochondrial-specific prodrug for treating glioblastoma. Mol. Cancer Ther. 19:2445–2453.

Rong, M., A. Matsuda, Y. Hiraoka, and J. Lee. 2016. Meiotic cohesin subunits RAD21L and REC8 are positioned at distinct regions between lateral elements and transverse filaments in the synaptonemal complex of mouse spermatocytes. J. Reprod. Dev. 62:623–630.

Ruan, H., Y. Li, X. Wang, B. Sun, W. Fang, S. Jiang, and C. Liang. 2020. CRYAB inhibits migration and invasion of bladder cancer cells through the PI3K/AKT and ERK pathways. Jpn. J. Clin. Oncol. 50:254–260.

Schafler, E. D., P. A. Thomas, S. Ha, Y. Wang, K. Bermudez-Hernandez, Z. Tang, D. Fenyö, M. Vigodner, and S. K. Logan. 2018. UXT is required for spermatogenesis in mice. PLoS One 13:e0195747.

Shukla, V., J. B. Kaushal, P. Sankhwar, M. Manohar, and A. Dwivedi. 2019. Inhibition of TPPP3 attenuates β-catenin/NF-κB/COX-2 signaling in endometrial stromal cells and impairs decidualization. J. Endocrinol. 240:417–429.

Song, X., X. Wan, T. Huang, C. Zeng, N. Sastry, B. Wu, C. D. James, C. Horbinski, I. Nakano, W. Zhang, B. Hu, and S. Y. Cheng. 2019. SRSF3-regulated RNA alternative splicing promotes glioblastoma tumorigenicity by affecting multiple cellular processes. Cancer Res. 79:5288–5301.

Tang, S., B. Yin, J. Xu, and E. Bao. 2018. Rosemary reduces heat stress by inducing CRYAB and HSP70 expression in broiler chickens. Oxid. Med. Cell. Longev. 2018:7014126.

Teng, K., S. Wei, C. Zhang, J. Chen, J. Chen, K. Xiao, J. Liu, M. Dai, X. Guan, J. Yun, and D. Xie. 2019. KIFC1 is activated by TCF-4 and promotes hepatocellular carcinoma pathogenesis by regulating HMGA1 transcriptional activity. J. Exp. Clin. Cancer Res. 38:329.

Tesfay, H. H., Y. Sun, Y. Li, L. Shi, J. Fan, P. Wang, Y. Zong, A. Ni, H. Ma, A. I. Mani, and J. Chen. 2020. Comparative studies of semen quality traits and sperm kinematic parameters in relation to fertility rate between 2 genetic groups of breed lines. Poult. Sci. 99:6139–6146.

Thomas, P. A., E. D. Schafler, S. E. Ruff, M. Voisin, S. Ha, and S. K. Logan. 2020. UXT in Sertoli cells is required for blood-testis barrier integrity†. Biol. Reprod. 103:880–891.

Vyklicka, L., and P. V. Lishko. 2020. Dissecting the signaling pathways involved in the function of sperm flagellum. Curr. Opin. Cell Biol. 63:154–161.

Wang, C., Y. T. Zeng, X. Y. Chen, Q. Y. Wu, L. Q. Yang, L. Xu, Y. Zhang, I. H. Qazi, G. B. Zhou, C. J. Zeng, Z. Z. Zuo, T. Z. Song, Q. Zhu, and M. Zhang. 2019. Improvac induces immunocastration by affecting testosterone levels and disrupting spermatogenesis in male broiler chickens. Poult. Sci. 98:6034–6345.

Wei, Y. L., T. Yang, T. Kovacs, and W. X. Yang. 2019. C-terminal kinesin motor es-KIFC1 regulates nuclear formation during spermiogenesis in Chinese mitten crab Eriocheir sinensis. Gene 719:144074.

Winston, N.J., M.H. Johnson, J.M. McConnell, D.I. Cook, and MLJ Biology of reproduction Day. 2004. 'Expression and role of the ether-à-go-go-related (MERG1A) potassium-channel protein during preimplantation mouse development', 70: 1070-1079.

Xiao, Y. X., H. Q. Shen, Z. Y. She, L. Sheng, Q. Q. Chen, Y. L. Chu, F. Q. Tan, and W. X. Yang. 2017. C-terminal kinesin motor KIFC1 participates in facilitating proper cell division of human seminoma. Oncotarget 8:61373–61384.

Xiyang, Y. B., R. Liu, X. Y. Wang, S. Li, Y. Zhao, B. T. Lu, Z. C. Xiao, L. F. Zhang, T. H. Wang, and J. Zhang. 2020. COX5A plays a vital role in memory impairment associated with brain aging via the BDNF/ERK1/2 signaling pathway. Front. Aging Neurosci. 12:215.

Xu, H., M. D. Beasley, W. D. Warren, G. T. van der Horst, and M. J. McKay. 2005. Absence of mouse REC8 cohesin promotes synapsis of sister chromatids in meiosis. Dev. Cell 8:949–961.

Xu, L., Q. Guo, G. Chang, L. Qiu, X. Liu, Y. Bi, Y. Zhang, H. Wang, W. Lu, L. Ren, Y. Chen, Y. Zhang, Q. Xu, and G. Chen. 2017. Discovery of microRNAs during early spermatogenesis in chicken. PLoS One 12:e0177098.

Yang, EK, K Takimoto, Y Hayashi, WC de Groat, and NJ Neuroscience Yoshimura. 2004. 'Altered expression of potassium channel subunit mRNA and alpha-dendrotoxin sensitivity of potassium currents in rat dorsal root ganglion neurons after axotomy', 123: 867-874.

Ye, K., Y. Li, W. Zhao, N. Wu, N. Liu, R. Li, L. Chen, M. He, B. Lu, X. Wang, and R. Hu. 2017. Knockdown of tubulin polymerization promoting protein family member 3 inhibits cell proliferation and invasion in human colorectal cancer. J. Cancer 8:1750–1758.

Zalazar, L., C. Stival, A. R. Nicolli, G. A. De Blas, D. Krapf, and A. Cesari. 2020. Male decapacitation factor SPINK3 blocks membrane hyperpolarization and calcium entry in mouse sperm. Front. Cell Dev. Biol. 8:575126.

Zhang, J., J. Liu, J. Wu, W. Li, Z. Chen, and L. Yang. 2019. Progression of the role of CRYAB in signaling pathways and cancers. Oncol. Targets Ther. 12:4129–4139.

Zuo, Q., J. Jin, K. Jin, C. Sun, J. Song, Y. Zhang, G. Chen, and B. Li. 2019. Distinct roles of retinoic acid and BMP4 pathways in the formation of chicken primordial germ cells and spermatogonial stem cells. Food Funct. 10:7152–7163.